Delft University of Technology

The role of sky view factor and urban street greenery in human thermal comfort and heat stress in a desert climate

Ahmadi Venhari, Armaghan; Tenpierik, Martin; Taleghani, Mohammad

Important note
To cite this publication, please use the final published version (if applicable).
Please check the document version above.

The role of sky view factor and urban street greenery in human thermal comfort and heat stress in a desert climate

Abstract

The aim of this study was to understand the effect of urban street greenery type and arrangements on thermal comfort and heat stress in summer. Field measurements and computer simulations were carried out on East-West (E-W) and North-South (N-S) oriented streets in Isfahan, Iran. Through the field measurements in July 2014, 17 different streets were studied, followed by 15 perturbation scenarios (urban design alternatives) simulated by ENVI-met. The study showed that there is a significant and positive relationship between the Sky View Factor (SVF) and the Physiological Equivalent Temperature (PET) values. Comparison of the meteorological parameters within different street orientations showed that the effect of the SVF on the E-W streets was more significant than in N-S streets. Furthermore, greenery arrengement and building heights showed different impacts on the outdoor thermal comfort streets with different orientations.

Keywords:

Thermal comfort, heat stress, urban greenery, sky view factor, urban streets, desert climate.

1. Introduction

Human thermal comfort represents a state of mind that expresses satisfaction with the thermal environment (ISO-7730, 2005). Traditional thermal comfort theory was based on the balance between heat production and heat loss to keep the core body temperature at around 37 °C (Nikolopoulou and Lykoudis, 2006, Van Hoof, 2008). As thermal comfort is affected by different environmental factors like air temperature, wind speed, humidity and mean radiant temperature, it requires an overall view of human-biometeorological conditions. Thermal comfort consists of six factors; two personal (metabolic rate (Met) and thermo-physical properties of clothing (Clo)); and four environmental factors (air temperature (T_a), mean radiant temperature (T_{mrt}), air velocity (V_a) and relative humidity (RH)) (Mayer, 1993).

There are different human-biometeorological indexes. Physiological Equivalent Temperature (PET) has been used in several studies to evaluate the human thermal comfort in outdoor environments (Höppe, 1999, Mayer and Höppe, 1987). Several advantages are associated with the popularity of PET, like involving clothing and metabolic rate in the calculations, and using °C as a tangible unit of measurement (Deb and Alur, 2010). In a desert climate with high air temperature and low humidity in summertime, the human-biometeorological conditions not only cause discomfort, but also severe heat stress could happen for pedestrians. It means that the body cannot maintain its core temperature at around 37 °C, which is harmful for elderly and people with cardiovascular problems (Sampson et al., 2013, Robine et al., 2008, Kabisch et al., 2017).

Several heat mitigation strategies are used to decrease thermal stress and improve thermal comfort in urban areas. Adding urban greenery is one of the well-known strategies (Vanos et al., 2019, Saaroni et al., 2018, Lee et al., 2016, Lee and Mayer, 2018). As mentioned in many studies, shading (Shashua-Bar and Hoffman, 2000, Kotzen, 2003, Saaroni et al., 2018, Mayer et al., 2008, Holst and Mayer, 2011, Lee et al., 2013, Lee et al., 2014), evaporation (Montazeri et al., 2015), and transpiration (Fryd et al., 2011, Oliveira et al., 2011, Taleghani, 2018) cause the cooling effect of urban greenery. In contrast to the urban heat island effect, the term "Urban Cool Island" (UCI) is used when an area in a city is cooled down by a heat mitigation strategy like urban greenery (Hamada and Ohta, 2010). When the cooling effect is due to urban greenery, the term Green Cooling Island (GCI) is used (Taha et al., 2016). Yang et al. (2011) studied the effect of urban design strategies on thermal comfort. They observed PET reduction up to 20 °C under the shadow of casting trees above pavements. In Sao Paolo, a reduction in PET of up to 12 °C was found due to street greenery (Spangenberg et al., 2008). Toudert and Mayer (2007) reported a reduction in PET of more than 20 °C. Furthermore, climate is an important factor that determines GCI. The effectiveness of urban greenery is more appreciable in hot climates (Shashua-Bar and Hoffman, 2002, Bowler et al., 2010). In a recent study in Iraq, the results showed that shading by trees increased the outdoor thermal comfort dramatically (Ridha et al., 2018). Two studies in 2017 presented that the GCIs in arid and semi-arid climates are more effective than other climates. Furthermore, the number of studies in these climates are limited (Ahmadi Venhari et al., 2017, Kleerekoper et al., 2017).

Iran has diverse climates. There are limited days in a year which meet thermal comfort conditions (Daneshvar et al., 2013). Roshan et al. (2017) determined new threshold temperatures for cooling and heating degree days index for different parts of Iran. The results showed that southern coasts and central plateau of Iran have more Cooling Degree Days (CDD) and need maximum cooling energy. One of the passive design strategies recommended in such climates is human-biometeorological oriented design (Snir et al., 2016, Middel et al., 2019, Taleghani et al., 2019, Zamani et al., 2012). Solar radiation, wind speed and evaporation are three important factors of climate design in such desert climates. Greenery is one of the most effective elements of a human-biometeorological oriented design which plays an important role in improving thermal comfort (Middel et al., 2015, Taleghani and Berardi, 2018, Lee et al., 2016, Lee and Mayer, 2018). There are many studies that showed the heat mitigation impacts of vegetation in traditional courtyards (Foruzanmehr and Vellinga, 2011, Nasrollahi et al., 2017, Taleghani et al., 2012), and in urban scale (Akbari and Kolokotsa, 2016, Yan et al., 2018) in arid climates. Due to the water shortage in such climates, urban greenery needs to be designed in the most efficient way.

Urban streets occupy the largest areas among urban spaces in cities (Jacobs, 1961). This is more common in compact cities like Iranian cities. Greening such large areas could significantly alter the urban climate. The main objective of this study is to understand how to design urban greenery for N-S and E-W streets. A previous study in Cuba illustrated that the heat stress is not the same in streets with different directions. In E-W streets, the heat stress was more than other directions (Rodríguez-Algeciras et al., 2018). There are several methods to find the most effective amount of shading trees. One of the most popular ones is based on the calculation of the sky view factor (SVF). SVF is defined as the percentage of free sky at a specific location (Oke, 2002), which ranges from 0 (completely obstructed) to 1 (completely open to the sky). By adding buildings and vegetation, the view to the sky could be blocked. As many studies illustrated, decreasing the SVF can reduce air temperature during the day (Svensson, 2006, Unger, 2004, Lee et al., 2014). Similar results show a direct relationship between SVF and PET in winter and summer (Lin et al., 2010, Charalampopoulos et al., 2013). This study will answer the following questions:

- What is the effect of green SVF and built SVF on pedestrian thermal comfort (based on the direction of streets)?
- What is the effect of SVF on streets in Isfahan?
- What greenery arrangement is more effective for E-W streets and N-S streets?
- How is the importance of the shading greenery in comparison with non-shading greenery on thermal comfort?

2. Methodology

This paper studies the effect of urban street greenery on pedestrians' thermal comfort. As mentioned in the introduction, different micrometeorological parameters influence thermal comfort like air temperature (T_a), mean radiant temperature (T_{mrt}), relative humidity (RH) and wind speed as well as personal factors. This study used PET as the thermal comfort index. The

effect of the built environment (height to width ratio in street canyons; H/W), urban greenery and SVF on thermal comfort were studied. The amount of green coverage was calculated from satellite images. For the ENVI-met simulations, building SVF and tree SVF were reported, separately. SVF was calculated with the RayMan software package (Matzarakis et al., 2010, Lee and Mayer, 2016). Lee and Mayer (2016) discussed that several studies have validated T_{mrt} with RayMan; however, these studies are mainly based on simulations. In their study, they validated RayMan results for T_{mrt} and PET with measured data for the first time (Lee and Mayer, 2016). They could show that RayMan "satisfactorily" simulates T_{mrt} under homogeneous conditions; however, the accuracy decreases with lower solar elevation.

2.1. The study area

The historical city of Isfahan is one of the largest cities in Iran with a population of 1.9 million in 493.8 km^2. Local latitude is 32'65°N, longitude 51'66°E and the elevation is approximately 1590 m above sea level. Isfahan has a desert climate (Köppen-Geiger BWk) with high air temperature and low humidity during the summer, and cold desert climate in winter (Kottek et al., 2006). This climate is also known as an arid climate, as the precipitation is between 25 to 200mm per year. Desert climates divide to hot desert climate (BWh- like Tucson (Arizona) and Cairo (Egypt)), and cold desert climate (BWk like central Iranian cities like Isfahan, and Santiago (Chile)). Yaghmaei et al. (2009) studied the human-biometeorological conditions of Isfahan province based on Koppen (2006) climate classification. These methods have been compared and a multivariate statistical method has been suggested. They showed that the city of Isfahan has a windy, arid and warm climate. Based on global warming and some wrong decisions in water management in Iran, Isfahan has been confronted with drought and the main river of the city, Zayandehrood, has dried up. By comparing the mean monthly temperature of July 2000 till 2015, the increase in air temperature over the last decade is more than 3°C (geographic.org, 2017).

2.2. Field study

To select the streets for this study, a surface temperature map was prepared by Envi 4.7 based on the Landsat 7 data (Figure 1). As a result, 4 districts were chosen. The hottest district in the
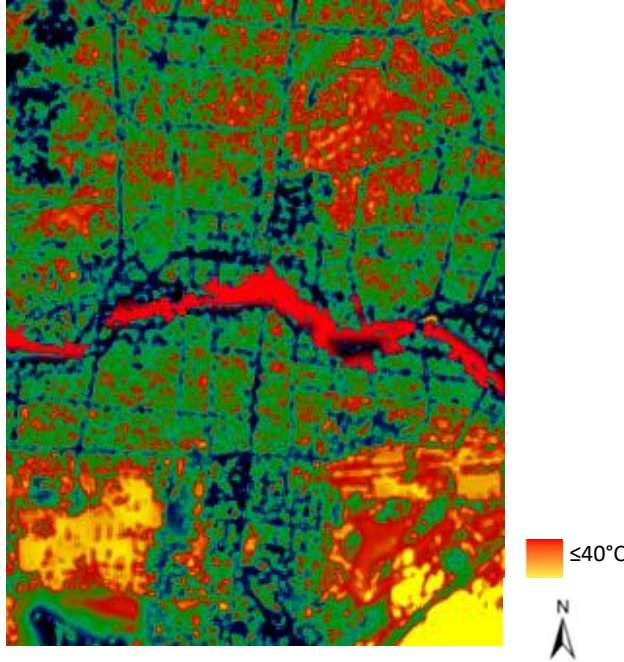

Figure 1: Thermal surface simulation of Isfahan,

20 July 2013

Figure 2: The location of selected districts for field study in the city of Isfahan

historical fabric (Dis 1); the coolest district (Dis 2); and two other districts, one in a new fabric and another located between the old and the new fabric in Isfahan. Figure 2 shows the selected districts. In each district, 3 to 8 streets were chosen with either N-S or E-W streets. The streets have different amounts of urban greenery, H/W and greenery arrangements (Table 2). In District 2, the number of selected streets is more than the other districts due to the existing different greenery arrangements. Based on the method which has been applied by Shashua-Bar and Hoffman (2002), in each street several points with a distance of about 20 m were studied. To make the data comparable, a reference point was selected in each district. This reference point did not have any vegetation or shading during the day. Data were not collected during the windy days. The wind velocity was less than 0.5 m/s in all days during which data was gathered. Measurements were performed from 20th to 25th July 2014 at 8:00, 13:00, 17:00 and 22:00 at the height of 1.4 m above the ground. Table 1 presents the specification of the measurement devices. A black globe with diameter equal to 15 cm was used to measure T_g. T_{mrt} was then calculated by Equation 1 (ISO7726, 1998):

$$T_{mrt} = \left[\left(T_g + 273.15 \right)^4 + 2.5 \cdot 10^8 \cdot V_a^{0.6} \left(T_g - T_a \right) \right]^{1/4} - 273.15 \qquad (1)$$

where;

T_{mrt} is mean radiant temperature,

T_g is globe temperature,

V_a is wind speed, and

T_a is air temperature.

5

Table 1: Devices used in the field studies.

Variable	Unit	Devices	Accuracy	Method of storage	Calibrated company	Applied points
Air Temperature (T$_a$)	°C	Kestrel 4500	0.1°C±	Automatic	Kestrel Meters	Reference points
		Kimo-VT100-1	0.3°C±	Manual	KIMO instrument	Site measurements
		Heat index WBGT meter 8758	0.6°C±	Manual	UMTC	Site measurements
Humidity	%	EasyLog. EL-USC-2-LCD	±3%	Automatic	Lascar Electronics	Reference point and Site measurements
Wind Velocity	m/s	Kimo-VT100-1	0.05±	Manual	KIMO instrument	Site measurements
		Kestrel 4500	0.1±	Manual	Kestrel Meters	Site measurements
Globe Temperature (T$_g$)	°C	Heat index WBGT meter 8758	1.5°C±	Manual	UMTC	Site measurements
Surface Temperature (T$_s$)	°C	Infrared FLIR E4 Camera	-	Automatic	FLIR instrument	Site measurements

In each point of the streets, a fish eye photo was taken. A Sony Cyber Shot DSC-H7 with 42xHD lens and 800dpi resolution was employed to take the fish eye photos. By inputting these fish eye photos and other meteorological data in RayMan 1.2, the SVF and PET were calculated. For each street, the differences between the observation points and the reference points are represented by ΔT_a, ΔT_s, ΔT_{mrt}, and ΔPET.

Figure 3: Devices used in the field study.

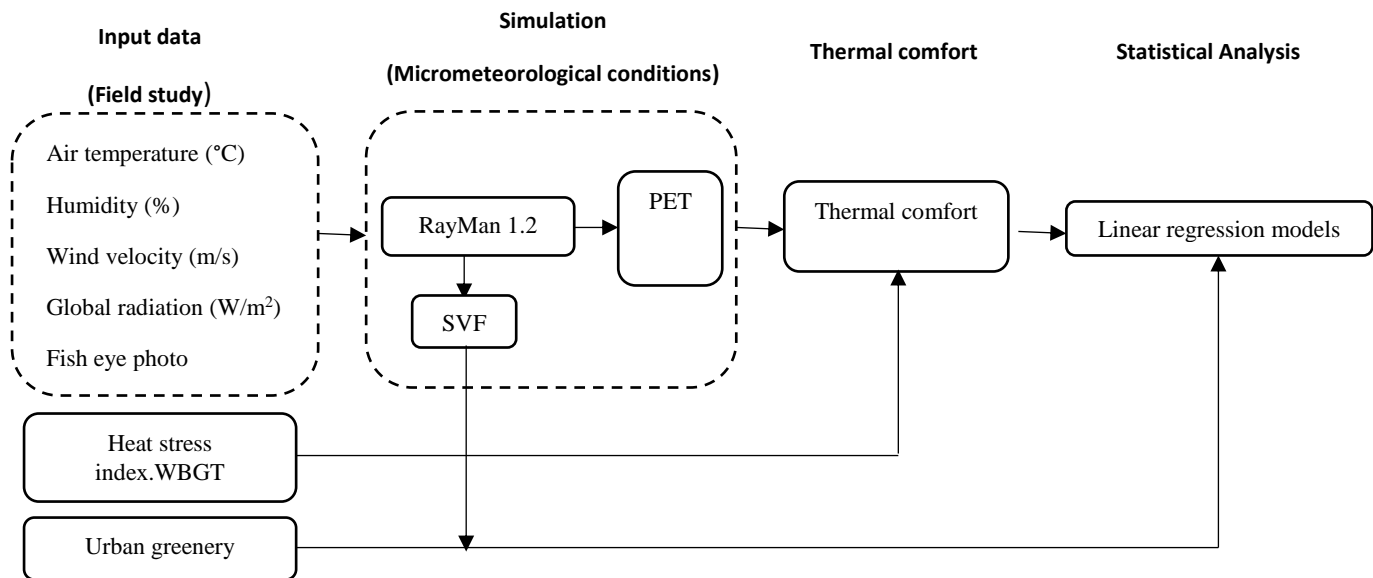Figure 4 illustrates the research method used for the field studies.

178

Figure 4: Research method in field study

Table 2: Site data and measurement plan.

District	Street	Number of observation points	Street direction	Green coverage (%)	Average SVF	Width of streets(m)
1	Abdorazzagh	30	N-S	19	0.67	**35**
	Hatef	21	N-S	27	0.56	**25**
	Moshirodole	16	E-W	0	0.62	**15**
2	Cheharbagh. A	30	N-S	67	0.41	**43**
	Shaykh Bahai	21	E-W	38.5	0.59	**20**
	Shams Abadi	21	N-S	34	0.61	**25**
	Alam Ala	15	E-W	91	0.33	**12**
	Amadegah	18	E-W	37	0.46	**20**
	Bagh Goldaste	21	N-S	1	0.82	**35**
	Niasarm	21	E-W	94	0.22	**20**
	Abas Abad	18	E-W	82	0.28	**15**
3	Shaykh sadugh	24	N-S	58	0.58	**35**
	Azadi	42	E-W	42	0.6	**30**
	Freiburg	28	N-S	11	0.76	**35**
4	Daghighi	18	E-W	9	0.73	**35**
	Nayej	18	N-S	85	0.54	**20**
	Khaghani	18	E-W	25	0.41	**15**

183

2.2. Simulation

In stage 2 of the research, ENVI-met 3.1 was employed (Bruse, 2004, Bruse and Fleer, 1998). This software is used for three dimensional micrometeorological simulations. Its typical spatial resolution is between 0.5 to 10m. ENVI-met simulates air and surface temperatures (°C), relative humidity (%), wind velocity (m/s) and mean radiant temperature (°C) (Bruse, 2019). Fluid dynamics and thermodynamics are the bases to simulate heat, vapour and air flows at different levels. The grid size used for the simulations were $2 * 2 * 2$ m^3 (x * y * z). ENVI-met has been previously used in different studies that focused on urban greenery (Wong et al., 2007, Fabbri et al., 2017, Lee and Mayer, 2016, Lee and Mayer, 2018).

In this stage of the study, five different alternatives were simulated (Alt1 to Alt5 shown in Figure 5). These alternatives had different amounts and arrangements of greenery in a 25 m wide street in Isfahan. Meteorological data of the 4th district was used as the input because of the common form of its streets in Isfahan. In addition, these five alternatives were studied for three different heights of the adjacent buildings: H/W equal to 1/1, 1/2, 1/4.
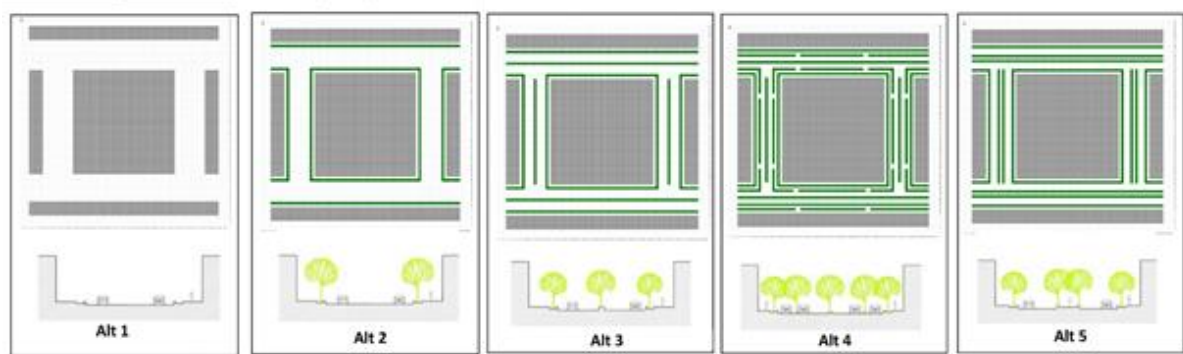

Figure 5: Five alternatives with different amount and arrangements of greenery which have been simulated in ENVI-met.

For each simulation, four receptors in the E-W and four receptors in the N-S streets recorded the simulated meteorological data. Fifteen simulation scenarios with 16 receptors (in each model) were run for a 24-hour period during the 20th of July 2014. Meteorological data at the height of 1.4 m from receptors were extracted (like the measurement campaign). This height was chosen as it is closest to the human body core (Ali-Toudert and Mayer, 2006). In addition, the first alternative scenario without greenery was considered as the reference model. PET reduction for each alternative is calculated from the average PET differences of the receptor

209 points in the simulation models. Figure 6 illustrates a summary of the research method for the
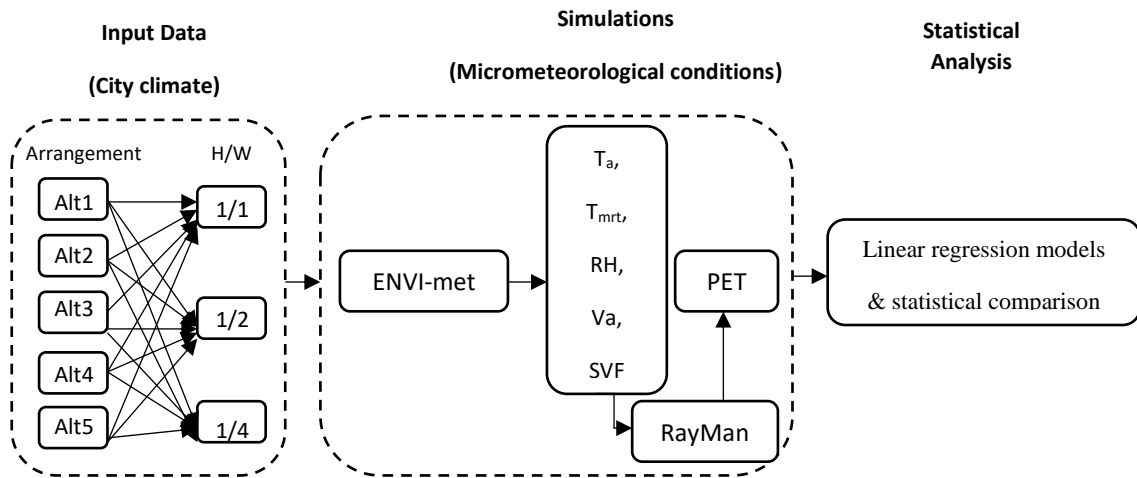210 simulations.

Figure 6: Research method in simulations.

211

212

3. Results and discussion:

3.1.The effect of sky view factor (SVF) on thermal comfort

215 To find out the amount of solar radiation within urban spaces, linear regression analyses were
216 done between the different GCI parameters and SVF. Table 5 presents the average differences
217 of T_a, T_s, T_{mrt} and PET between the measurement points and the reference points that have been
218 used in the regression analyses.

219
220 Table 3: The average difference of thermal indexes between measurement points and the reference point

221

ΔPET (°C)	ΔT$_{mrt}$ (°C)	ΔT$_s$ (°C)	ΔT$_a$ (°C)	Street	District
1.4	-4.3	-1. 8	1.1	Abdorazzagh	**1**
1.7	-9.9	-5. 6	2.0	Hatef	
2.2	-0.2	0.5	0.6	Moshirodole	
-1.1	-10.4	-7.5	-2.2	Cheharbagh. A	2
0.9	-5.5	-3.9	-0.6	Shaykh Bahai	
-0.9	-5	-1.7	1.1	Shams Abadi	
-1.1	-12.3	-9.4	-5.0	Alam Ala	
-1.1	-10.2	-6.4	-2.2	Amadegah	
3.7	-0.3	0.4	1.6	Bagh Goldaste	
-3.1	-13.4	12.4	-7.0	Niasarm	
-2.1	-13.6	-7.6	-6.3	Abas Abad	
2.0	-5.7	-4.5	-1.4	Shaykh sadugh	3
-2.6	-4.4	-3.7	3.8	Azadi	
3.1	-1.7	0. 6	1.9	Fribourg	
1.6	-2.2	0.4	1.6	Daghighi	4
-2.3	-13.9	-7.5	-4.5	Nayej	
0.8	-12.4	-8.6	6 .3	Khaghani	

231 First, all streets regardless of their direction were included in the analysis to see the effect of
232 SVF on ΔT$_a$, ΔT$_s$, ΔT$_{mrt}$ and ΔPET. As can be seen in Figure 6, the effect of SVF on air
233 temperature is not appreciable, however, its effect on thermal comfort (PET), T_s and T_{mrt} is
234 notable. Because of other factors like land use, the limited effect of SVF on T_a is explainable.

For example, in Azadi street, a park is near the street which affects the ambient air temperature. Because of these factors, the coefficient of determination (R^2) for this relationship is also smallest (54%). This means that 54% of the variations in ΔT_a is explained by the corresponding variations in SVF. The largest effect of SVF was found on ΔT_s, with a slope of the regression line of 23.6 °C per unit change in SVF (R^2=0.71), which means that the direct effect of SVF on surface temperatures. The largest coefficient of determination was found between ΔT_{mrt} and SVF (R^2=0.84). This indicates that 84% of the variations in ΔT_{mrt} is explained by changes in the SVF. Due to the intense solar radiation in desert climates, the necessity of controlling solar radiation availability can be clearly seen. Furthermore, it was observed that minimum (0.22) and maximum (0.82) SVF led to 10.2°C difference in PET. In addition, the results of the regression analyses show a significant positive relationship between SVF and PET.
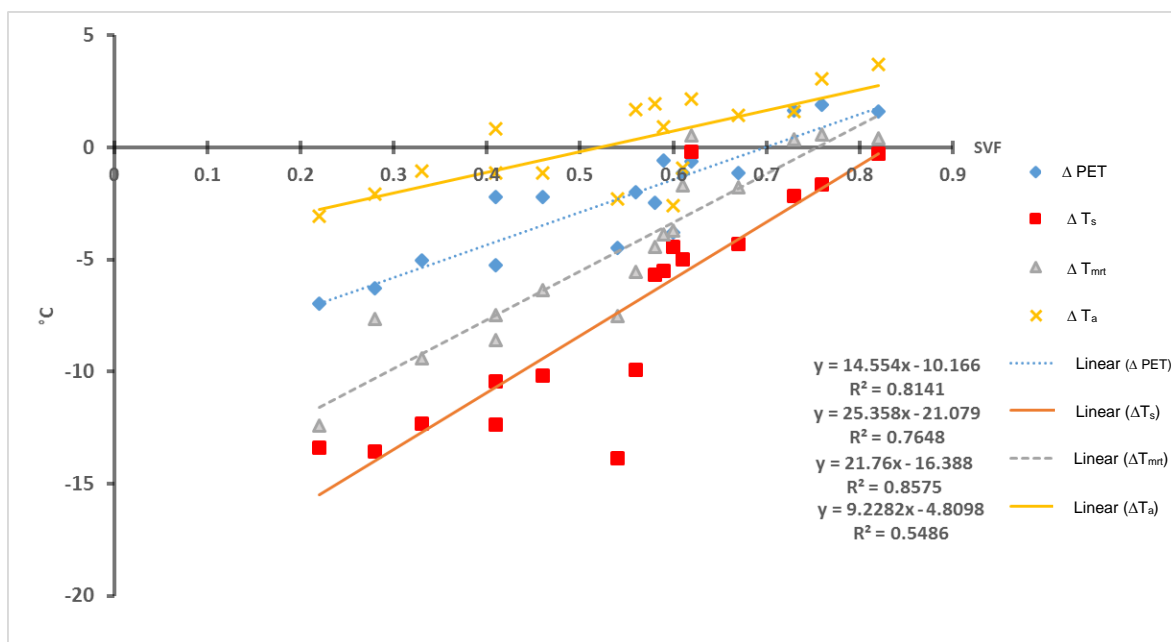

Figure 7: The linear regression model for the relation between SVF and thermal indexes without street direction.

The next part of the comparison is focused on the street directions. As Table 6 presents, based on the slope of the regresion lines (b), the SVF affects the air temperature in N-S streets more than in E-W ones. In addition, PET is more affected by SVF in E-W streets than in N-S ones. In general, PET was higher in E-W streets compared to the N-S streets. Decreasing SVF has a stronger cooling effect (on PET) in E-W streets. This is in accordance with the previous studies that showed the effectiveness of shading from urban greenery (Shashua-Bar and Hoffman, 2000, Holst and Mayer, 2011, Lee et al., 2016, Lee and Mayer, 2018).

Table 4: Results of regresion analysis between thermal indexes and SVF based on direction (a is intercept; b is slope; r is correlation coefficient).

Direction	N-S			E-W		
	a	b	r	a	b	R

ΔT_a (°C)	-6.948	12.805	0.76	-4.08	7.7725	0.64
ΔT_s (°C)	-19.809	26.266	0.93	-23.554	28.509	0.83
ΔT_{mrt} (°C)	-15.978	22.918	0.93	-16.938	22.15	0.91
ΔPET (°C)	-9.2476	13.31	0.82	-10.12	14.947	0.92

The ENVI-met results showed that the effect of the SVF on air temperature was smaller than its effect on other micrometeorological factors. A 0.1 unit increase in SVF led to an increase of 1.6 °C and 2.4 °C air temperature in N-S and E-W streets, respectively. The effect of the SVF on T_{mrt} was found to be stronger (Figure 7). A 0.1 unit increase in SVF led to 17.9 °C and 16.7 °C increase of mean radiant temperature within N-S and E-W streets, respectively. Among different micrometeorological parameterss, mean radiant temperature was more affected by changing the amount of greenery. The effect of the SVF on T_{mrt} in E-W streets seems to be quite similar to N-S streets. In general, T_{mrt} is about 6.0 °C higher in streets with E-W orientation than in streets with N-S orientation (with equal SVF). The reason can be that E-W streets are insolated from early morning, and they warm up sooner than N-S streets.

As the regression model illustrates (Figure 8), the effect of SVF on thermal comfort can emphasise the importance of shading. Shading trees and the shadow of buildings are very effective in this climate.
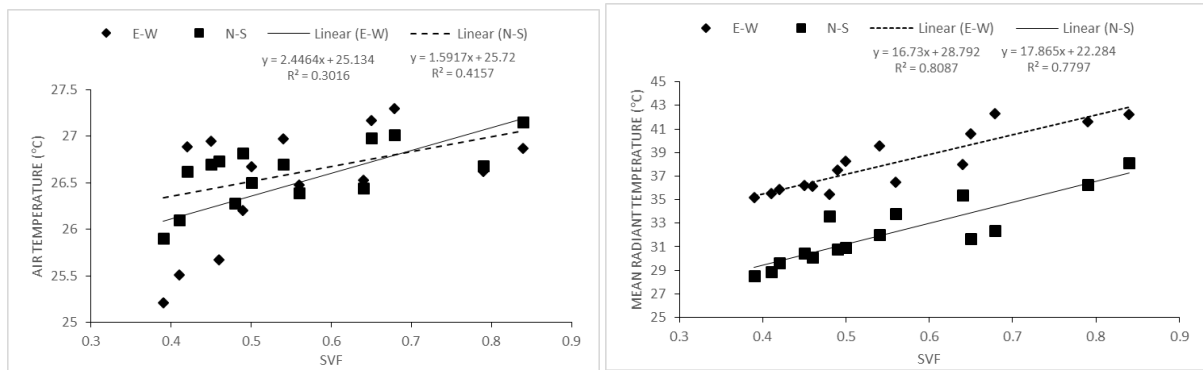

Figure 8: The regression model of the cooling effect of SVF with street direction based on simulations.

3.2 The cooling effect of street greenery arrangement, H/W ratio, and Greenery arrangement

To explore the cooling effect of different street greenery arrangements, RayMan was used to calculate the PET after the ENVI-met simulations. Comparing the different greenery arrangements, the maximum GCI (in PET) was 13.6 °C. This shows the important role of greenery arrangements in providing outdoor thermal comfort. To understand the cooling effect

of different alternatives, average PET was compared. Alt 1 (with no greenery) was used as the reference model. By adding shading trees (Figure 9), 4 °C reduction in the average PET was observed. In N-S streets, the difference between Alt-2 with two lines of greenery, and Alt 3 with three lines of greenery was about 0.6 °C. This PET reduction in E-W streets is 1.5 °C. It can be concluded that adding shading trees at the middle of the E-W streets is an effective arrangement to improve the pedestrians' thermal comfort. The most effective alternative for both directions is Alt 4 which is dividing the streets into different lines for pedestrians, transition and traffic with in-between shading trees. As a result, in desert climates a lower SVF with streets divided by shading trees is an effective method to improve outdoor thermal comfort.

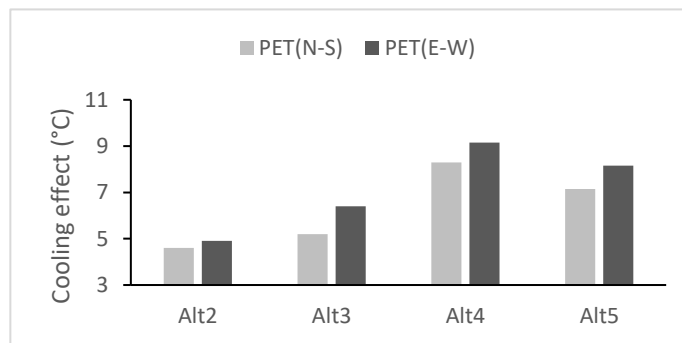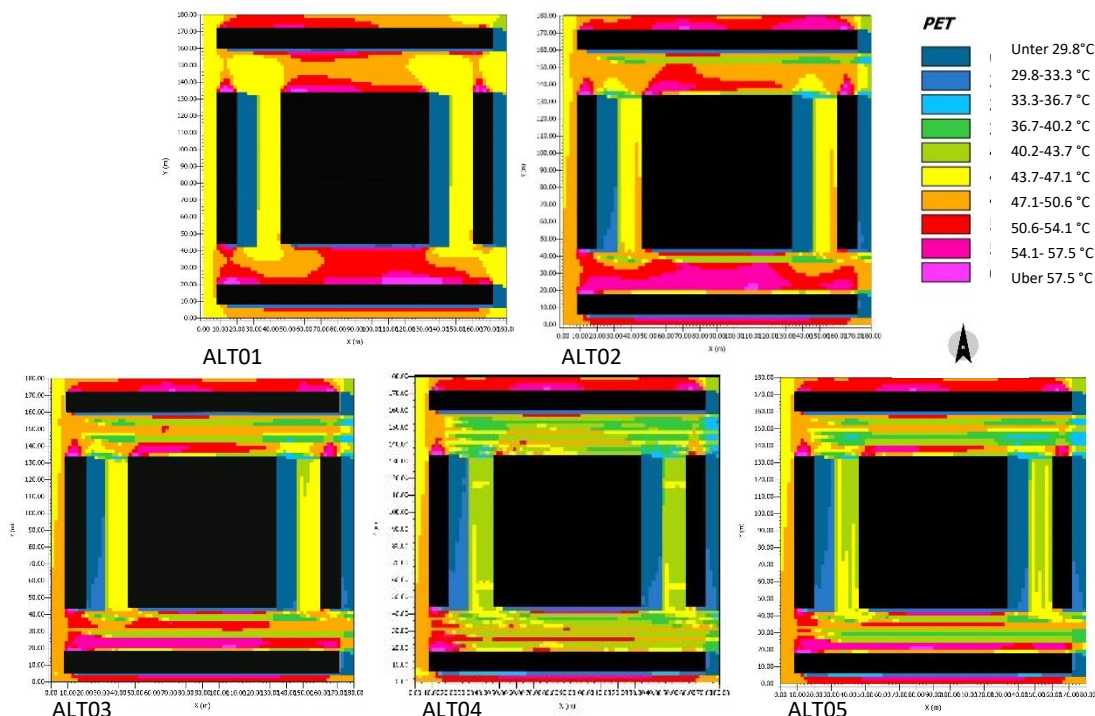Figure 9: The cooling effect of studied alternatives in simulations, based on the average of PET.

Figure 10: An example of PET simulations by ENVI-met in 13:00 (figures are generated by Leonardo, a component of ENVI-met).

Type of greenery: Trees have a stronger impact on PET reduction than grass. For example, Fribourg street can be divided into two parts. Both parts have three lines of greenery, but the

first part is with shading trees; and the second part is with grass on two sides, and grass and bushes in the middle. Figure 11 shows the change in air temperature as compared to the bare reference for 28 measurement points along the street. As the figure shows, the cooling effect of the first part (lower receptor numbers), especially at around noon, is more than of the second part (higher receptor numbers). E, W and C represent the east, west and centre of the street. The results show the importance of shadow in this desert climate. Considering the water shortage, shading trees play more important role in improving the thermal comfort than non-shading vegetation.
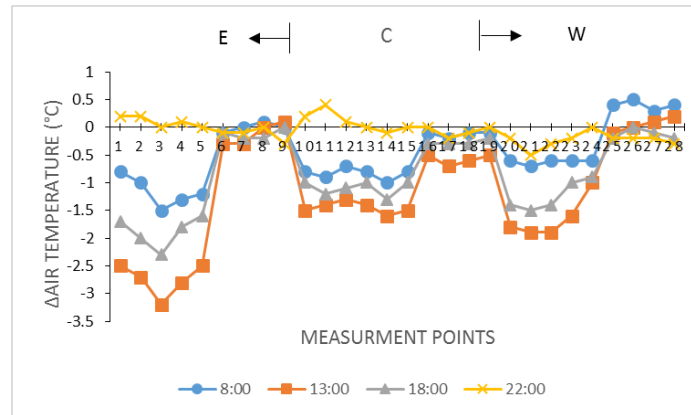

Figure 11: The cooling effect of urban greenery in the middle and two sides of the street.

H/W ratio: Simulating different alternatives for three different building heights was the last part of this study. Figure 12 shows the results of mean radiant temperature in 15 simulations. As the figure shows, increasing the H/W ratio in N-S streets is more effective than in E-W streets. In N-S streets, by increasing the H/W ration from 1/4 to 1/2, a maximum reduction in T_{mrt} of about 14.4 °C was achieved, while the maximum effect in E-W streets was 4.3 °C. The effect of increasing the H/W ratio from 1/4 to 1/2 was more significant that changing it from 1/2 to 1. Therefore, the recommended H/W ratio for the N-S streets is around 1/2. This result showed that blocking about half of the sky is very effective for heat mitigation. It should be noted that in N-S streets, blocking more than 1/2 of the sky not only has a small cooling effect but also may decrease natural ventilation in the streets.
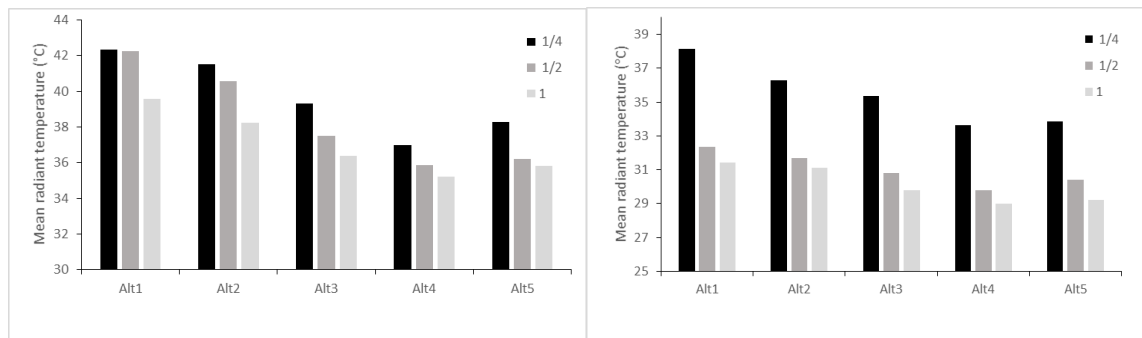

Figure 12: T_{mrt} in five different H/W scenarios in N-S (left) and E-W streets (right).

13

4. Conclusions

This study investigated urban street greenery as a strategy to reduce heat stress and to improve thermal comfort in outdoor environments. Field studies and computer simulations were carried out. The analyses were based on the local meteorological conditions of Isfahan in July 2014. In this climate, water shortage is a problem. Finding strategies which help landscape and urban designers take the most efficient decisions was the aim of this research. The effect of SVF, street greenery arrangement and H/W ratio of streets on heat mitigation were studied with different scenarios. The orientations of the investigated streets were North-South and East-West. The main findings of the paper are presented as follow:

- In the first phase of this study, the relation between the SVF and different micrometeorological factors were studied through field measurements. A regression analysis showed that the effect of SVF on air temperature was smallest, while its effect on mean radiant temperature and surface temperature were the largest. In addition, a positive and significant relationship was obtained between SVF and PET.
- A comparison of the effect of the greenery types illustrated that not all greenery lead to the same cooling effect. The maximum cooling effect is caused by the shadow of trees. Long lines of grass and bushes are not recommended for the arid climate of Isfahan. Shading trees which their crown cover each other are the most effective forms of greenery to reduce SVF, and consequently PET.
- Comparing the minimum (0.22) and maximum (0.82) SVFs, led to 10.2 °C difference in PET. In addition, sky obstruction in E-W streets reduced PET more than in N-S streets. This means that not every street needs the same amount of greenery. In E-W streets, controlling the incoming solar radiation is very important.
- Different alternatives of greenery arrangement led to maximum 13.7 °C reduction in PET. This showed the effect of greenery arrangement on outdoor thermal comfort. In addition, dividing streets into different lines with shading trees has the highest effect for heat stress mitigation. In E-W streets, a row of trees in the centre of the street is very effective to improve the pedestrian's thermal comfort. In addition, increasing the height of the buildings in the N-S streets plays an important role in heat stress mitigation. This effect was not notable in the E-W streets. As a result, increasing greenery in the E-W streets, and increasing the H/W ratio in the N-S streets are the two main recommended strategies for desert climates.

References

AHMADI VENHARI, A., TENPIERIK, M. & MAHDIZADEH HAKAK, A. 2017. Heat mitigation by greening the cities, a review study. *Environment, Earth and Ecology,* 1**,** 5-32.

AKBARI, H. & KOLOKOTSA, D. 2016. Three decades of urban heat islands and mitigation technologies research. *Energy and Buildings,* 133**,** 834-842.

ALI-TOUDERT, F. & MAYER, H. 2006. Numerical study on the effects of aspect ratio and orientation of an urban street canyon on outdoor thermal comfort in hot and dry climate. *Building and Environment,* 41**,** 94-108.

374 ALI-TOUDERT, F. & MAYER, H. 2007. Effects of asymmetry, galleries, overhanging façades and
375   vegetation on thermal comfort in urban street canyons. *Solar Energy,* 81**,** 742-754.
376 BOWLER, D. E., BUYUNG-ALI, L., KNIGHT, T. M. & PULLIN, A. S. 2010. Urban greening to cool towns
377   and cities: A systematic review of the empirical evidence. *Landscape and Urban Planning,* 97**,**
378   147-155.
379 BRUSE, M. 2004. ENVI-met 3.0: Updated Model Overview. http://www.envi-
380   met.net/documents/papers/overview30.pdf.
381 BRUSE, M. 2019. *ENVI-met website* [Online]. Available: http://www.envimet.com [Accessed].
382 BRUSE, M. & FLEER, H. 1998. Simulating surface–plant–air interactions inside urban environments
383   with a three dimensional numerical model. *Environmental Modelling & Software,* 13**,** 373-
384   384.
385 CHARALAMPOPOULOS, I., TSIROS, I., CHRONOPOULOU-SERELI, A. & MATZARAKIS, A. 2013. Analysis
386   of thermal bioclimate in various urban configurations in Athens, Greece. *Urban Ecosystems,*
387   16**,** 217-233.
388 DANESHVAR, M. R. M., BAGHERZADEH, A. & TAVOUSI, T. 2013. Assessment of bioclimatic comfort
389   conditions based on Physiologically Equivalent Temperature (PET) using the RayMan Model
390   in Iran. *Central European Journal of Geosciences,* 5**,** 53-60.
391 DEB, C. & ALUR, R. 2010. *The significance of Physiological Equivalent Temperature (PET) in outdoor*
392   *thermal comfort studies*.
393 FABBRI, K., CANUTI, G. & UGOLINI, A. 2017. A methodology to evaluate outdoor microclimate of the
394   archaeological site and vegetation role: A case study of the Roman Villa in Russi (Italy).
395   *Sustainable Cities and Society,* 35**,** 107-133.
396 FORUZANMEHR, A. & VELLINGA, M. 2011. Vernacular architecture: questions of comfort and
397   practicability. *Building Research & Information,* 39**,** 274-285.
398 FRYD, O., PAULEIT, S. & BÜHLER, O. 2011. The role of urban green space and trees in relation to
399   climate change. *CAB Reviews: Perspectives in Agriculture, Veterinary Science, Nutrition and*
400   *Natural Resources,* 6**,** 1-18.
401 GEOGRAPHIC.ORG. 2017. Available:
402   https://geographic.org/global_weather/iran/esfahan_shahid_beheshti_intl_408000_99999.
403   html [Accessed 15.01.2017].
404 HAMADA, S. & OHTA, T. 2010. Seasonal variations in the cooling effect of urban green areas on
405   surrounding urban areas. *Urban Forestry & Urban Greening,* 9**,** 15-24.
406 HOLST, J. & MAYER, H. 2011. Impacts of street design parameters on human-biometeorological
407   variables. *Meteorologische Zeitschrift,* 20**,** 541-552.
408 HÖPPE, P. 1999. The physiological equivalent temperature - A universal index for the
409   biometeorological assessment of the thermal environment. *International Journal of*
410   *Biometeorology,* 43**,** 71-75.
411 ISO7726 1998. International Standard 7726. *Ergonomics of the thermal environment - Instrument for*
412   *measuring physical quantities.* Geneva: ISO
413 ISO-7730 2005. ISO 7730 2005-11-15 Ergonomics of the Thermal Environment: Analytical
414   Determination and Interpretation of Thermal Comfort Using Calculation of the PMV and PPD
415   Indices and Local Thermal Comfort Criteria. ISO.
416 JACOBS, J. 1961. *The Death and Life of Great American Cities*, Vintage Books.
417 KABISCH, N., VAN DEN BOSCH, M. & LAFORTEZZA, R. 2017. The health benefits of nature-based
418   solutions to urbanization challenges for children and the elderly – A systematic review.
419   *Environmental Research,* 159**,** 362-373.
420 KLEEREKOPER, L., TALEGHANI, M., VAN DEN DOBBELSTEEN, A. & HORDIJK, T. 2017. Urban measures
421   for hot weather conditions in a temperate climate condition: A review study. *Renewable and*
422   *Sustainable Energy Reviews,* 75**,** 515-533.
423 KOTTEK, M., GRIESER, J., BECK, C., RUDOLF, B. & RUBEL, F. 2006. World Map of the Köppen-Geiger
424   climate classification updated. *Meteorologische Zeitschrift,* 15**,** 259-263.

425 KOTZEN, B. 2003. An investigation of shade under six different tree species of the Negev desert
426   towards their potential use for enhancing micro-climatic conditions in landscape
427   architectural development. *Journal of Arid Environments,* 55**,** 231-274.
428 LEE, H., HOLST, J. & MAYER, H. 2013. Modification of Human-Biometeorologically Significant Radiant
429   Flux Densities by Shading as Local Method to Mitigate Heat Stress in Summer within Urban
430   Street Canyons. *Advances in Meteorology,* 2013**,** 13.
431 LEE, H. & MAYER, H. 2016. Validation of the mean radiant temperature simulated by the RayMan
432   software in urban environments. *International Journal of Biometeorology,* 60**,** 1775-1785.
433 LEE, H. & MAYER, H. 2018. Maximum extent of human heat stress reduction on building areas due to
434   urban greening. *Urban Forestry & Urban Greening,* 32**,** 154-167.
435 LEE, H., MAYER, H. & CHEN, L. 2016. Contribution of trees and grasslands to the mitigation of human
436   heat stress in a residential district of Freiburg, Southwest Germany. *Landscape and Urban*
437   *Planning,* 148**,** 37-50.
438 LEE, H., MAYER, H. & SCHINDLER, D. 2014. Importance of 3-D radiant flux densities for outdoor
439   human thermal comfort on clear-sky summer days in Freiburg, Southwest Germany.
440   *Meteorologische Zeitschrift,* 23**,** 315-330.
441 LIN, T.-P., MATZARAKIS, A. & HWANG, R.-L. 2010. Shading effect on long-term outdoor thermal
442   comfort. *Building and Environment,* 45**,** 213-221.
443 MATZARAKIS, A., RUTZ, F. & MAYER, H. 2010. Modelling radiation fluxes in simple and complex
444   environments: basics of the RayMan model. *Int J Biometeorol,* 54**,** 131-9.
445 MAYER, H. 1993. Urban bioclimatology. *Experientia,* 49**,** 957-963.
446 MAYER, H., HOLST, J., DOSTAL, P., FLORIAN, I. & SCHINDLER, D. 2008. Human thermal comfort in
447   summer within an urban street canyon in Central Europe. *Meteorologische Zeitschrift,* 17**,**
448   241-250.
449 MAYER, H. & HÖPPE, P. 1987. Thermal comfort of man in different urban environments. *Theoretical*
450   *and Applied Climatology,* 38**,** 43-49.
451 MIDDEL, A., CHHETRI, N. & QUAY, R. 2015. Urban forestry and cool roofs: Assessment of heat
452   mitigation strategies in Phoenix residential neighborhoods. *Urban Forestry & Urban*
453   *Greening,* 14**,** 178-186.
454 MIDDEL, A., LUKASCZYK, J., ZAKRZEWSKI, S., ARNOLD, M. & MACIEJEWSKI, R. 2019. Urban form and
455   composition of street canyons: A human-centric big data and deep learning approach.
456   *Landscape and Urban Planning,* 183**,** 122-132.
457 MONTAZERI, H., BLOCKEN, B. & HENSEN, J. L. M. 2015. Evaporative cooling by water spray systems:
458   CFD simulation, experimental validation and sensitivity analysis. *Building and Environment,*
459   83**,** 129-141.
460 NASROLLAHI, N., HATAMI, M., KHASTAR, S. R. & TALEGHANI, M. 2017. Numerical evaluation of
461   thermal comfort in traditional courtyards to develop new microclimate design in a hot and
462   dry climate. *Sustainable Cities and Society,* 35**,** 449-467.
463 NIKOLOPOULOU, M. & LYKOUDIS, S. 2006. Thermal comfort in outdoor urban spaces: Analysis across
464   different European countries. *Building and Environment,* 41**,** 1455-1470.
465 OKE, T. R. 2002. *Boundary Layer Climates,* London, Taylor & Francis.
466 OLIVEIRA, S., ANDRADE, H. & VAZ, T. 2011. The cooling effect of green spaces as a contribution to
467   the mitigation of urban heat: A case study in Lisbon. *Building and Environment,* 46**,** 2186-
468   2194.
469 RIDHA, S., GINESTET, S. & LORENTE, S. 2018. Effect of the Shadings Pattern and Greenery Strategies
470   on the Outdoor Thermal Comfort. *International Journal of Engineering and Technology,* 10**,**
471   108-114.
472 ROBINE, J.-M., CHEUNG, S. L. K., LE ROY, S., VAN OYEN, H., GRIFFITHS, C., MICHEL, J.-P. &
473   HERRMANN, F. R. 2008. Death toll exceeded 70,000 in Europe during the summer of 2003.
474   *Comptes Rendus Biologies,* 331**,** 171-178.

475 RODRÍGUEZ-ALGECIRAS, J., TABLADA, A. & MATZARAKIS, A. 2018. Effect of asymmetrical street
476   canyons on pedestrian thermal comfort in warm-humid climate of Cuba. *Theoretical and*
477   *Applied Climatology,* 133**,** 663-679.
478 ROSHAN, G. R., FARROKHZAD, M. & ATTIA, S. 2017. Defining thermal comfort boundaries for heating
479   and cooling demand estimation in Iran's urban settlements. *Building and Environment,* 121**,**
480   168-189.
481 SAARONI, H., AMORIM, J. H., HIEMSTRA, J. A. & PEARLMUTTER, D. 2018. Urban Green Infrastructure
482   as a tool for urban heat mitigation: Survey of research methodologies and findings across
483   different climatic regions. *Urban Climate,* 24**,** 94-110.
484 SAMPSON, N. R., GRONLUND, C. J., BUXTON, M. A., CATALANO, L., WHITE-NEWSOME, J. L., CONLON,
485   K. C., O'NEILL, M. S., MCCORMICK, S. & PARKER, E. A. 2013. Staying cool in a changing
486   climate: Reaching vulnerable populations during heat events. *Global Environmental Change,*
487   23**,** 475-484.
488 SHASHUA-BAR, L. & HOFFMAN, M. E. 2000. Vegetation as a climatic component in the design of an
489   urban street: An empirical model for predicting the cooling effect of urban green areas with
490   trees. *Energy and Buildings,* 31**,** 221-235.
491 SHASHUA-BAR, L. & HOFFMAN, M. E. 2002. The Green CTTC model for predicting the air
492   temperature in small urban wooded sites. *Building and Environment,* 37**,** 1279-1288.
493 SNIR, K., PEARLMUTTER, D. & ERELL, E. 2016. The moderating effect of water-efficient ground cover
494   vegetation on pedestrian thermal stress. *Landscape and Urban Planning,* 152**,** 1-12.
495 SPANGENBERG, J., SHINZATO, P., JOHANSSON, E. & DUARTE, D. 2008. Simulation of the influence of
496   vegetation on microclimate and thermal comfort in the city of Sao Paulo. *Revista da*
497   *Sociedade Brasileira de Arborização Urbana (REVSBAU),* 3**,** 1-19.
498 SVENSSON, M. K. 2006. Sky view factor analysis – implications for urban air temperature differences.
499   *Meteorological Applications,* 11**,** 201-211.
500 TAHA, H., WILKINSON, J., BORNSTEIN, R., XIAO, Q., MCPHERSON, G., SIMPSON, J., ANDERSON, C.,
501   LAU, S., LAM, J. & BLAIN, C. 2016. An urban-forest control measure for ozone in the
502   Sacramento, CA Federal Non-Attainment Area (SFNA). *Sustainable Cities and Society,* 21**,** 51-
503   65.
504 TALEGHANI, M. 2018. Outdoor thermal comfort by different heat mitigation strategies- A review.
505   *Renewable and Sustainable Energy Reviews,* 81**,** 2011-2018.
506 TALEGHANI, M. & BERARDI, U. 2018. The effect of pavement characteristics on pedestrians' thermal
507   comfort in Toronto. *Urban Climate,* 24**,** 449-459.
508 TALEGHANI, M., CRANK, P. J., MOHEGH, A., SAILOR, D. J. & BAN-WEISS, G. A. 2019. The impact of
509   heat mitigation strategies on the energy balance of a neighborhood in Los Angeles. *Solar*
510   *Energy,* 177**,** 604-611.
511 TALEGHANI, M., TENPIERIK, M. & DOBBELSTEEN, A. 2012. The Effect of Different Transitional Spaces
512   on Thermal Comfort and Energy Consumption of Residential Buildings. *7th Windsor*
513   *Conference: The changing context of comfort in an unpredictable world Cumberland Lodge.*
514   Windsor, UK: Network for Comfort and Energy Use in Buildings.
515 UNGER, J. 2004. Intra-urban relationship between surface geometry and urban heat island: review
516   and new approach. *Climate Research,* 27**,** 253-264.
517 VAN HOOF, J. 2008. Forty years of Fanger's model of thermal comfort: comfort for all? *Indoor Air,* 18**,**
518   182-201.
519 VANOS, J. K., KOSAKA, E., IIDA, A., YOKOHARI, M., MIDDEL, A., SCOTT-FLEMING, I. & BROWN, R. D.
520   2019. Planning for spectator thermal comfort and health in the face of extreme heat: The
521   Tokyo 2020 Olympic marathons. *Science of The Total Environment,* 657**,** 904-917.
522 WONG, N. H., KARDINAL JUSUF, S., AUNG LA WIN, A., KYAW THU, H., SYATIA NEGARA, T. & XUCHAO,
523   W. 2007. Environmental study of the impact of greenery in an institutional campus in the
524   tropics. *Building and Environment,* 42**,** 2949-2970.

525   YAGHMAEI, L., SOLTANI, S. & KHODAGHOLI, M. 2009. Bioclimatic classification of Isfahan province
526   using multivariate statistical methods. *International Journal of Climatology,* 29**,** 1850-1861.
527   YAN, H., WU, F. & DONG, L. 2018. Influence of a large urban park on the local urban thermal
528   environment. *Science of The Total Environment,* 622-623**,** 882-891.
529   YANG, F., LAU, S. S. Y. & QIAN, F. 2011. Thermal comfort effects of urban design strategies in high-
530   rise urban environments in a sub-tropical climate. *Architectural Science Review,* 54**,** 285-304.
531   ZAMANI, Z., TALEGHANI, M. & HOSEINI, S. B. 2012. Courtyards as solutions in green architecture to
532   reduce environmental pollution. *Energy Education Science & Technology, Part A: Energy*
533   *Science and Research,* 30**,** 358-396.

534